

Finite Element Investigations on Temperature and Residual Stresses during Machining Ti6Al4V Alloy using TiAlN Coated Plain and Textured Tools

Sarvesh Kumar Mishra, Sudarsan Ghosh, Sivanandam Aravindan*

Department of Mechanical Engineering, Indian Institute of Technology- Delhi, New Delhi, 110016

Abstract

The present study investigates the effect of textured tools on cutting temperature and residual stresses in machining of titanium alloys through simulations. 2D and 3D finite element (FE) simulations have been carried out to understand the role of TiAlN coating and tool rake face texturing on generation of cutting temperature and residual stresses. The simulations show that lower temperature got generated in machining with textured TiAlN tools and also resulted in reduced tensile residual stresses in the machined workpiece.

Keywords: FEM, Residual stresses, textured tools

1. INTRODUCTION

Titanium alloys have been proved to be the workhorse for the aerospace and automotive industries. Conventional titanium alloys such as Ti6Al4V account for nearly 30% of aero engine weight in commercial aircrafts. High tensile strength, high strength to weight ratio, better corrosion resistance favor its use in different sectors. Surface integrity of finished components after machining processes affects its operational life and usefulness in critical safety applications. Surface integrity of finished components accounts for surface roughness (Ra), residual stresses, and micro-hardness values at the surface and sub-surface regions. Surface roughness index below 0.4 μ m imposed by the aerospace sector for critical components can be achieved by machining operations using suitable lubri-coolant strategies (MQL, Cryo-coolants, etc.) [1]. But control of residual stresses in components with machining parameters is still a rigorous task to be performed.

The extent of residual stresses in machining processes is a topic of wide interest since the last few decades. These stresses (compressive and/or tensile in nature) can be generated due to the formation of a severe deformation gradient under the combined action of the mechanical, physical, thermal and metallurgical phenomenon in cutting zones [2]. These mentioned phenomena in machining process result in residual stresses to finished work material and affect each other interdependently. Plastic deformation is caused by the action of material removal (shearing) and rubbing between the tool and finished workpiece at flank face. Thermal gradients are caused by the intense rate of shear deformation in the primary shear zone, frictional heat at tool-chip (secondary zone) and tool-finished workpiece zone (tertiary zone). After machining process, residual stresses and their distribution in surface and sub-surface layers are the governing phenomena for the operational life of machined components. Residual stresses are also important for corrosion resistance and dimensional accuracy of the finished product. Tensile residual stresses generated on machined surface and sub-surface layers act as active sites for crack generation and stress corrosion cracking when in operation.

There exists a number of experimental and theoretical studies on residual stress evaluation of machined components produced by turning process [3]. These experimental techniques use a combination of machining experiments with statistical methods to develop empirical models for a particular range of machining parameters. But to develop these models, very cumbersome processes are followed to conduct machining trials

with costly and time consuming characterization methods (e.g., X-Ray Diffraction). With the advent of powerful computational systems, finite element methods (FEM) can be seen as a possible direction to predict residual stress generation and its distribution in machined components. Increasing literature on FEM based predictions has proposed finite element based methods as a strong tool to develop ways to relate different variables in machining operation with the generation of residual stresses and distribution with surface depth up to few microns.

Surface modifications of cutting tools have been suggested as an alternative for efficient machining process aiming dry cutting of steels and aluminum alloys. Some of the applications of textured tools have been found for hard to machine materials, e.g., hardened steels, titanium alloys. Surface textured tools, filled with soft coatings (MoS₂, WS₂, graphite, CaF₂, etc.), are getting increasingly used for these alloys. The present study looks into the applicability of hard ceramic TiAlN coatings on textured tools for machining of Ti6Al4V and their effect on cutting temperature and residual stresses. The temperature in machining zone affects the residual stresses due to thermal contribution on machined surface and subsurface. So, the tool temperature variation and temperature distribution in the machined zone during cutting are being studied by FE analysis.

2. 3D FINITE ELEMENT SIMULATIONS

FE simulation package (AdvantEdge® Version 7.3, Third Wave Systems, USA) was used for the evaluation of residual stresses in machining with plain and textured tools. 3D finite element studies were conducted for running simulations for plain and textured tools with and without TiAlN coatings. Simulations were performed in standard mode with residual stress analysis up to two layers of machined surface cut in standard mode.

Table 1 Johnson-Cook parameters for Ti6Al4V alloy [5]

J-C parameters	Value	Texture Parameters	
Yield strength (A)	782.7 MPa	Diameter	80 μ m
Hardening modulus (B)	498.4 MPa	Pitch	180 μ m
Hardening coefficient (n)	0.28	Depth	20 μ m
Strain rate sensitivity coefficient (C)	0.028	Distance from edge	120 μ m
Ref. plastic strain rate ($\dot{\epsilon}_0$)	1 s ⁻¹		
Room temperature (T ₀)	20°C		
Melting temperature (T _m)	1660°C		

User defined temperature dependent Johnson-Cook (modified J-C model) finite element model has been selected for the present study as this model is capable to describe material behavior at large machining strains and strain rates [4].

$$\sigma = (A + B.\varepsilon^n) \cdot \left[1 + C \cdot \ln \left(\frac{\dot{\varepsilon}}{\dot{\varepsilon}_0} \right) \right] \cdot \left[1 - \left(\frac{T - T_0}{T - T_m} \right)^m \right] \quad \dots(1)$$

The values of constitutive model parameters for Ti6Al4V are given in **Table 1**. Thermal softening coefficient (m) is kept as unity in this case. Mechanical properties of Ti6Al4V, WC/Co, and TiAlN coating material are presented in **Table 2**. The coefficient of friction for plain and TiAlN coated tools were kept 0.7 and 0.5 respectively.

Table 2 Mechanical and thermal input parameters

Properties	Ti6Al4V	WC/Co	TiAlN
Density (Kg/m ³)	4430	14,900	4700
Coefficient of thermal expansion (°C ⁻¹)	9.1E-6	4.8E-6	As of tool
Young's Modulus (Pa)	1.13*E11	6.45*E11	3.1*E11
Poisson ratio	0.34	0.24	0.22
Thermal conductivity (W.m ⁻¹ .C ⁻¹)	K(T)	91	16
Sp. heat(J.kg ⁻¹ .C ⁻¹)	C _p (T)	206	779

The workpiece is modeled with a volume of 1x2x5 mm³ and simulations have been run for a cutting length of 3 mm for all conditions. The workpiece is given a constant velocity corresponding to the cutting speed to provide relative motion for shearing. **Fig. 1** shows simulation set up with fully grown chips during the cutting operation and the texture dimensions on cutting tools. Temperature dependent heat capacity and thermal conductivity are used for better assessment of thermal softening nature.

Table 3 Temperature dependent properties of Ti6Al4V

Temperature(°C)	0	500	1000	1500
K(T)	6.651	8.591	15.031	22.286
C _p (T)	483.3	588.3	600.19	690.2

The simulations conducted for plain non textured cutting tools (plain and TiAlN coated) are validated by results of the experimental study conducted by Ozel et al. [6]. Based on that further simulations are carried for textured and coated textured tools.

3. RESULTS AND DISCUSSION

Fig 2 shows the temperature distribution on cutting tool rake face in case of plain and textured tools. The temperature near the tool edge is higher in case of plain uncoated tools [Fig.2 (a)]. Temperature is the lowest in case of textured TiAlN coated tools [Fig. 2(d)]. Cutting forces for all cases are compared and average cutting forces and average tool temperatures are shown in Fig. 3. Textured TiAlN coated tool usageresulted in the minimum main cutting force and average temperature generation as compared to plain, plain TiAlN and textured uncoated tools. The percentage reduction for F_x, F_y, F_z, and T_{avg} for the textured TiAlN tools compared to plain uncoated tools are 6.4%, 4.09%, 6.6% and 7.13% respectively.

Fig 4 shows temperature distribution in machining zone and chip underside for plain and textured tools (uncoated and TiAlN

coated). Maximum temperatures in the machining zones are 1088^oC, 917^oC, 1045^oC and 881^oC for plain, plain TiAlN, textured and textured TiAlN coated tools respectively. A substantially reduced machining zone temperature can be observed in case of machining with textured TiAlN tools. The reduction of machining zone temperature is approximately 19% compared to plain tools at the same parametric levels.

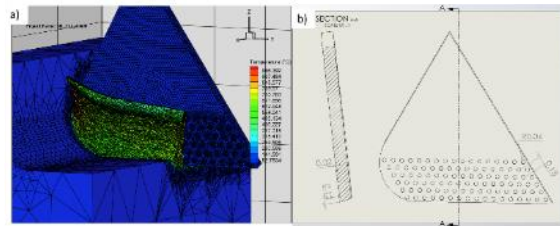


Fig. 1 (a) Simulation set up with fully grown chip and (b) dimensions of textured tools

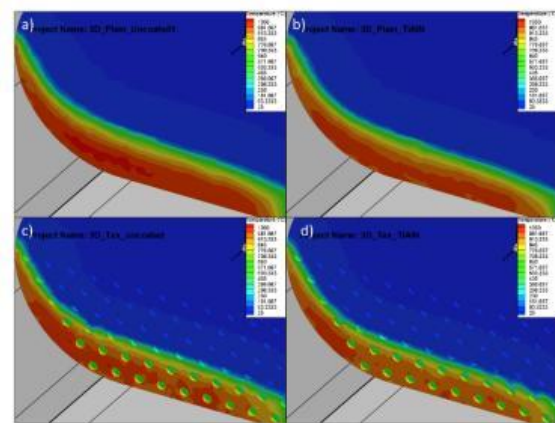


Fig. 2 Cutting temperature distribution on tool surfaces for (a) plain uncoated, (b) plain TiAlN, (c) textured uncoated and (d) textured TiAlN tools

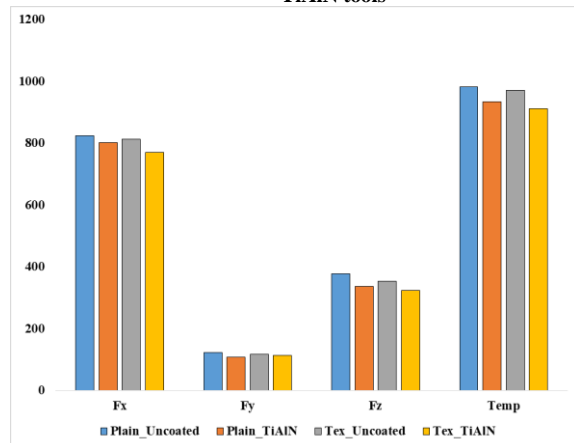


Fig. 3 Simulation results for average forces and cutting temperature

2D FE simulations are run for residual stress as shown in Fig. 5 for the same cutting conditions. Two pass analysis is done and results relating residual stresses are taken separately from 3-extraction zones (20%, 60%, and 95% from start position) as shown in Fig.5(b). The variation for residual stresses with depth from the surface is shown in Fig. 6(a). It shows that variation of residual stresses becomes fairly constant after two pass simulation. Simulations were carried with mesh refinement depth (d_{fm}) 0.5 mm in 2-pass cut.

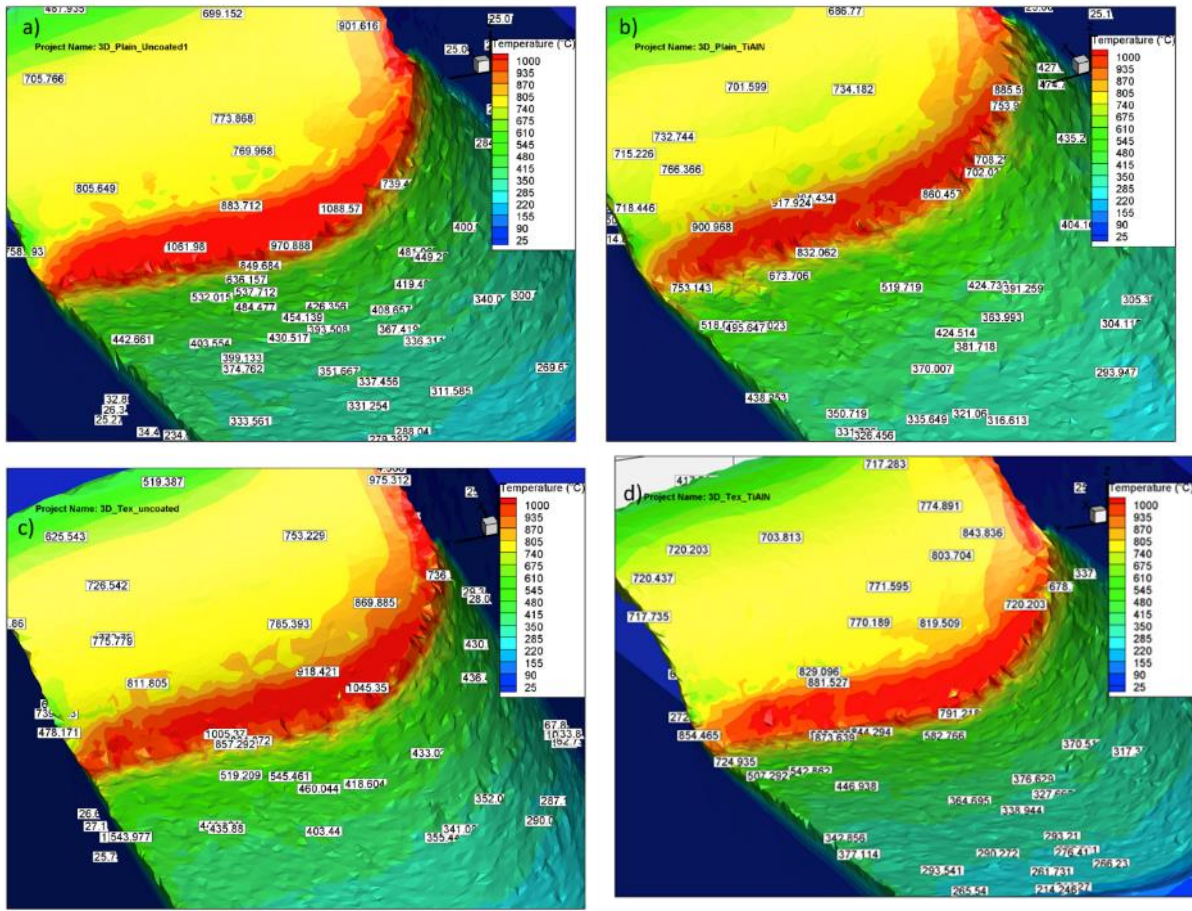


Fig. 4 Cutting zone temperature distribution for (a) plain uncoated, (b) plain TiAlN, (c) textured uncoated and (d) textured TiAlN tools

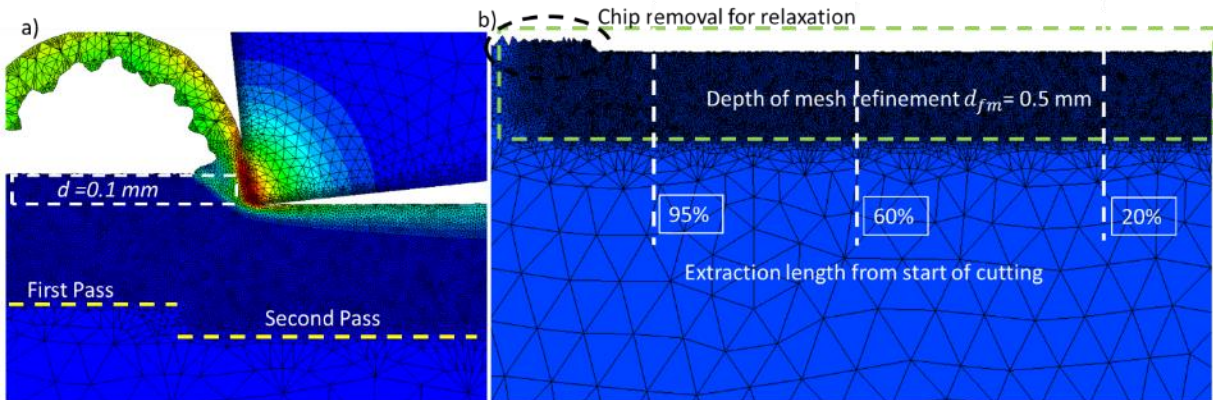


Fig. 5 Residual stress set up for (a) two pass simulation and (b) mesh refinement depth and relaxation

Fig. 6(b) and Fig. 6(c) shows the circumferential and axial stresses respectively in machined workpiece after cutting and relaxation step. The average of residual stresses at three different extraction zones [Fig. 5(b)] can be considered for further analysis. The variation of tensile and compressive stresses for axial and circumferential residual stresses are shown in Fig. 6(b)-(c).

The peak intensity of compressive stresses is plotted in Fig 7 for plain and textured tools respectively. The results in Fig. 7 show that the tensile residual stresses are absent only in the case of textured TiAlN tools. Peak compressive residual stress decreases for coated tools (plain and textured) compared to plain and textured uncoated tools.

4. CONCLUSIONS

The following conclusions may be drawn from the simulation studies:

1. Textured TiAlN coated tools reduces average cutting forces and cutting temperature on tools and in machining zone compared to plain and textured uncoated tools.
2. The peak intensity of residual stresses are higher for plain and textured uncoated tools compared to plain TiAlN and textured TiAlN tools.

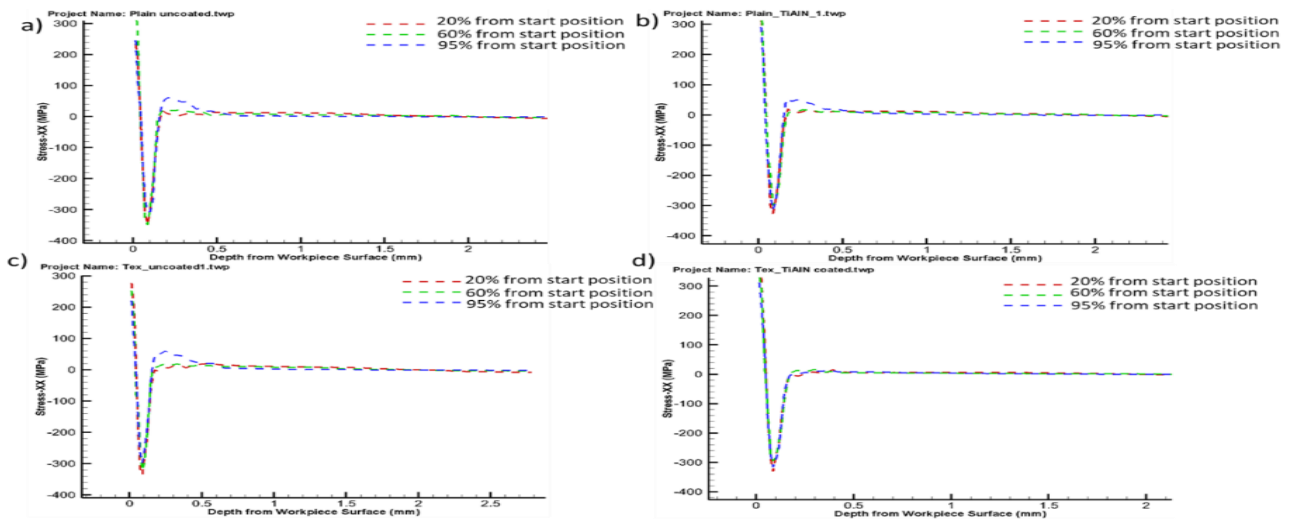


Fig. 7 Variation of residual stresses with surface depth at different cut length from start for (a) plain uncoated, (b) plain TiAlN, (c) textured uncoated and (d) textured TiAlN tools

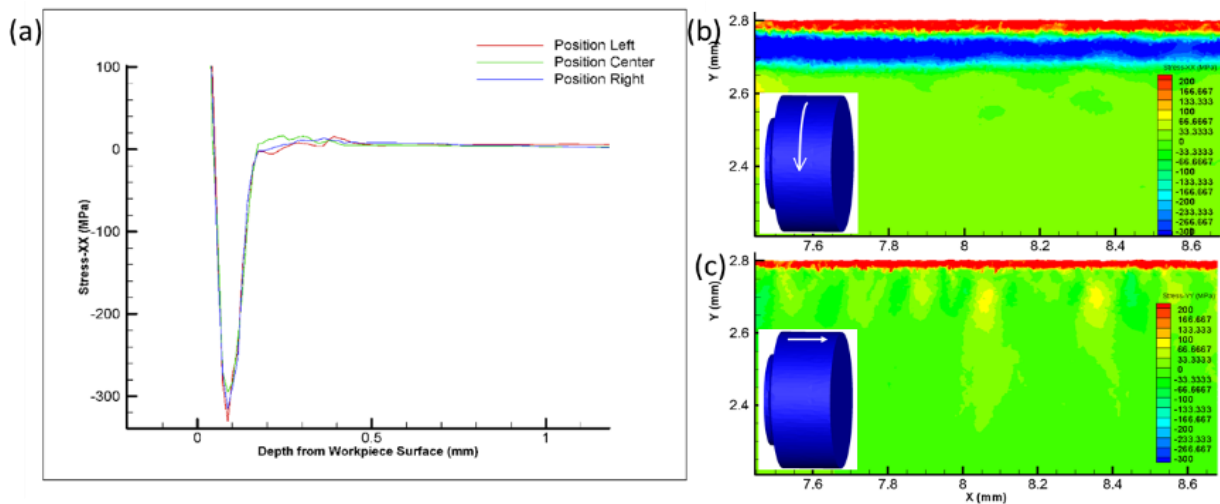


Fig. 6 Variation of residual stresses for (a) two-pass, (b) circumferential and (c) axial residual stresses on machined surfaces

3. Tensile residual stresses at some depth below the machined surface (depth = 200 μm from free surface) are absent in case of textured TiAlN coated tools. This may be attributed to lower machining zone temperature and lower tool temperature in case of textured TiAlN tools.
4. As evident from the simulation results, proper texturing on cutting tools may be beneficial for machining of Ti alloys in producing quality components devoid of tensile residual stresses.

References

- [1]. F. Klocke, D. Lung, M. Arft, P. C. Priarone, and L. Settineri, "On high-speed turning of a third-generation gamma titanium aluminide," *Int. J. Adv. Manuf. Technol.*, vol. 65, no. 1–4, pp. 155–163, 2013.
- [2]. E. Abboud, B. Shi, H. Attia, V. Thomson, and Y. Mebrahtu, "Finite element-based modeling of machining-induced residual stresses in Ti-6Al-4V under finish turning conditions," *Procedia CIRP*, vol. 8, pp. 63–68, 2013.
- [3]. M. Mohammadpour, M. R. Razfar, and R. Jalili Saffar, "Numerical investigating the effect of machining parameters on residual stresses in orthogonal cutting," *Simul. Model. Pract. Theory*, vol. 18, no. 3, pp. 378–389, 2010.
- [4]. D. Umbrello, "Finite element simulation of conventional and high speed machining of Ti6Al4V alloy," *J. Mater. Process. Technol.*, vol. 196, no. 1–3, pp. 79–87, 2008.
- [5]. T. Özel, M. Sima, A. K. Srivastava, and B. Kaftanoglu, "Investigations on the effects of multi-layered coated inserts in machining Ti-6Al-4V alloy with experiments and finite element simulations," *CIRP Ann. - Manuf. Technol.*, vol. 59, no. 1, pp. 77–82, 2010.
- [6]. [6] T. Özel and D. Uluhan, "Prediction of machining induced residual stresses in turning of titanium and nickel based alloys with experiments and finite element simulations," *CIRP Ann. - Manuf. Technol.*, vol. 61, no. 1, pp. 547–550, 2012.